GREEN SYNTHESIS OF NANO-SILVER/SODIUM ALGINATE/CARBOXYMETHYL XANTHAN GUM HYDROGEL AND EVALUATION OF ITS ANTI-INFLAMMATORY AND ANTI-*Helicobacter pylori* ACTIVITY

NOURA Y. ELMEHBAD,[*] NADIA A. MOHAMED,[**,***] NAHED A. ABD EL-GHANY[***] and MARWA M. ABDEL-AZIZ[****]

[*]*Department of Chemistry, Faculty of Science and Arts, Najran University, Najran, Saudi Arabia*
[**]*Department of Chemistry, College of Science, Qassim University, Qassim, Saudi Arabia*
[***]*Department of Chemistry, Faculty of Science, Cairo University, Giza, 12613, Egypt*
[****]*Regional Center for Mycology and Biotechnology, Al-Azhar University, Cairo, 11651, Egypt*
✉ *Corresponding author: N. A. Abd El-Ghany, abdelghanyn@sci.cu.edu.eg*

Received September 19, 2022

A crosslinked sodium alginate (SA)/carboxymethyl xanthan gum (CMXG) hydrogel was prepared by blending an equivalent weight ratio of SA and CMXG, followed by crosslinking using $CaCl_2$. Moreover, two nanocomposites were prepared by *in situ* dispersion of two different concentrations of silver nanoparticles (AgNPs) into the matrix of the prepared hydrogel. The analysis displayed that the order of COX-2 inhibition by the tested samples was SA < CMXG < crosslinked SA/CMXG hydrogel < SA/CMXG/AgNPs1% < SA/CMXG/AgNPs3% < Celecoxib. AgNP composites exhibited a potent inhibition tendency, and their activity increased with increasing the AgNPs content. The recorded MIC values revealed that the MIC values that cause 50% inhibition (IC_{50}) of COX-2 enzyme activity were 14.2 and 3.6 µg/mL for SA/CMXG/AgNPs1% and SA/CMXG/AgNPs3%, respectively, corresponding to 0.28 µg/mL for the standard drug Celecoxib. Moreover, SA/CMXG/AgNPs composites showed a greater inhibition efficiency of *H. pylori* than their parent SA/CMXG hydrogel. Their inhibitory efficiency increased with increasing their AgNPs content; SA/CMXG/AgNPs1% and SA/CMXG/AgNPs3% exhibited 100% inhibition against *H. pylori* growth at MIC of 3.9 and 1.95 µg/mL, respectively. The anti-*H. pylori* activity of SA/CMXG/AgNPs 3% was higher than that of the standard drug Clarithromycin, especially at the low concentrations ranging from 0.24 to 0.98 µg/mL. These results make SA/CMXG/AgNPs3% a promising anti-*H. pylori* agent.

Keywords: crosslinked sodium alginate/carboxymethyl xanthan gum hydrogel, silver nanoparticles, anti-inflammatory and *anti-Helicobacter pylori* activity

INTRODUCTION

Non-steroidal anti-inflammatory drugs (NSAIDs) have been widely used for treatment of fever and rheumatoid arthritis.[1-3] NSAIDs have pharmacological impacts that lead to inhibition of membrane enzyme Cyclooxygenase (COX). In the kidney, there are two isomers of COX; COX-1 and COX-2. COX-1 governs the essential functions of the cells and has a responsibility to produce the prostaglandin (PG) for protecting the kidney and gastrointestinal tract cells. So, its inhibition causes renal feebleness and peptic ulcer. Meanwhile, COX-2 is a proinflammatory enzyme that arises *via* inflammatory stimuli.[3,4] Thus, the selective inhibitors of the COX-2 participate in the beneficial anti-inflammatory properties of typical NSAIDs, without occurrence of damage effects on both the gastrointestinal tract and kidney.[5] So, many researchers have shown interest in finding out effective and selective inhibitors for COX-2, which can supply anti-inflammatory drugs associated with slight health risks, such as Celecoxib and SC-558.[3,5-7]

Helicobacter pylori (*H. pylori*) is a microaerophilic and neutrophilic spiral-shaped Gram-negative bacterial pathogen, associated with gastric diseases.[1,2] Infection by *H. pylori*

causes the direct or indirect dyspepsia, peptic ulcer disease, gastric mucosa-associated lymphoid tissue lymphoma, chronic gastritis, gastric adenocarcinoma and duodenal ulcer.[1] *H. pylori* catalyzes factors of growth, like inflammation modulators (COX-2) and granulocyte–macrophage colony-stimulating factor (GM-CSF).[8] The patients infected by *H. pylori* and the experimentally infected Mongolian gerbils suffered from increased expression of COX-2 within their gastric mucosa.[9] *H. pylori* activates the epidermal growth factor receptor (EGFR) in primary gastric epithelial cells, leading to an increase in the expression of COX-2. Enhancement of COX-2 expression leads to an increase in PGs secretion, resulting in death of the attenuated cells infected with *H. pylori*, which may contribute to carcinogenesis created *via* this pathogen over protracted time intervals of colonization.[10]

One of the priorities of current medicine and pharmacology researches is the investigation of the biological characteristics of metal nanoparticles associated with a considerable recent progress in nano-medicine and nano-pharmacology.[11] Now nano-technologies are used in the medicine practices for diagnosing, treating and preventing numerous diseases.[12] The drugs impregnated with silver nanoparticles (AgNPs) acquire a specific importance.[13] They have been utilized as anti-inflammatory and antiseptic agents for very long periods of time.[14] AgNPs are deemed to be one of the most important metal nanoparticles that display a distinguished inhibitory efficacy against various strains of pathogenic microorganisms, such as bacteria and fungi, and also showed antioxidant and anticancer effects.[15] They can be applied in coating the ceramic filters of water, wound dressings, cosmetic products, catheters, children's toys, air filters and antibacterial sprays,[16] creams and ointments for healing skin burns.[17] Generally, the large specific surface areas of AgNPs increase the contact regions between them and bacteria or fungi, enhancing remarkably the antimicrobial activities of AgNPs. However, some drawbacks appear during the practical application of AgNPs, the most important of which is the fabrication of the silver particles within a standard nano-size range, besides building up of stabilized colloidal systems, which prohibit the nanoparticles from agglomeration. Although searching for the most favorable stabilizer for nanoparticles is the most difficult mission, there are numerous routes for approaching it.[18] Due to biodegradability, biocompatibility and non-toxicity of natural polymers, these are more effective as stabilizers and dispersion media for AgNPs than synthetic polymers. Natural polymers, such as the structural polysaccharides of plants, are some of the most favorable stabilizers for a prospective use with AgNPs, in addition to their wide spectrum of biological properties.[19] The polysaccharide alginate, obtained from the seaweed, is an efficient stabilizer, which supplies high stabilization to AgNPs.[19] In recent years, AgNPs could be synthesized through green methods using natural polysaccharides, such as chitosan, alginate, agar and xanthan gum, which act as non-toxic reducing agents depending on the hydroxyl groups on their backbones.[20] To fully boost the antibacterial characteristics of AgNPs, their dispersion on the polymer surface without any aggregation should be achieved.[21]

Sodium alginate (SA) is a linear polysaccharide obtained from the marine algae. It is composed of different contents of α-L-guluronate and β-D-mannuronate linked by 1–4 glycosidic bonds. It possesses some interesting properties, such as water solubility, non-toxicity, biological compatibility and reproducibility.[22] SA can be converted into hydrogels or its insoluble polymers via the reaction with divalent and trivalent ions, particularly Ca(II) ions, to expand its usage in both food and non-food industries.[23]

Xanthan gum is the most commonly used gum as it is available and possesses outstanding rheological characteristics. It has other interesting properties as well, such as high viscosity even at low concentrations, a high degree of pseudo-plasticity, a wonderful solubility and stability at basic and acidic conditions and an excellent thermal stability at elevated temperatures.[24] It can be used in the food and cosmetic industries, in bioproducts and pharmaceutical formulations, as emulsifying and thickening agents for controlling both the micro-structure and texture, as well as for improving both the stability and the viscosity of ultimate products. Due to its functionality and unique structure, it could be applied in the biomedical domains, in comparison with the synthetic materials.[25]

SA, xanthan gum and carboxymethyl xanthan gum (CMXG) are useful biopolymers that can be used in the fabrication of biologically degradable films.[16] They can be applied in numerous domains, such as textiles, pharmaceutical and food industries.[26] Ag/gum and Ag/SA

nanocomposites were investigated for their antimicrobial activity in wound healing, water treatment and drug delivery, as biosensors and gas sensors.[16,20,22,24]

In the present work, to combine the advantages of AgNPs, SA and CMXG, we have prepared a crosslinked SA/CMXG hydrogel, using Ca(II) ions for the crosslinking process, to be used as a green reducing agent for $AgNO_3$ to produce AgNPs. The hydrogel restrains the aggregation of AgNPs, acts as a good stabilizer for the AgNPs and allows homogenous distribution of the AgNPs on and into the hydrogel matrix. The structure of the prepared hydrogel and its AgNP composites was characterized using FTIR spectroscopy, X-ray diffractometry, scanning electron microscopy, energy-dispersive X-ray spectroscopy and transmission electron microscopy. Furthermore, we investigated the anti-inflammatory and *anti-Helicobacter pylori* activity of the prepared hydrogel and its AgNP composites in order to examine their suitability to be used as potential materials for biomedical applications.

EXPERIMENTAL

Materials

Sodium alginate (SA) was purchased from Alpha-Chemika (India). Xanthan gum was obtained from Sigma-Aldrich (Germany). Sodium hydroxide, monochloroacetic acid, acetic acid, methanol and other chemicals were of analytical grade, provided by Aldrich, and used as received.

Methods

Preparation of carboxymethyl xanthan gum (CMXG)

Xanthan gum (1 g) was stirred in aqueous sodium hydroxide solution (20 mL, 7.5% w/v) at room temperature for 45 min to be swelled and alkalized. To the resulting suspension, monochloroacetic acid (1.5 g) dissolved in 10 mL of deionized water was gradually added under stirring. The temperature of the reaction was then raised to 70 °C and stirring was continued for 2 h. The resulting suspension was cooled and filtered. The product (CMXG) was immersed in methanol (85% v/v) overnight, neutralized to pH 7 using acetic acid, filtered, rinsed many times with methanol (85% v/v) and dried.[27]

Preparation of crosslinked SA/CMXG hydrogel

In brief, equal amounts of SA and CMXG (1 g) were added to 100 mL deionized water at room temperature and stirred well to form a homogeneous solution. The resulted polymer blend solution was crosslinked by gradual addition of $CaCl_2$ solution (50 mL, 0.05 mol/L) till complete precipitation was attained. The precipitated crosslinked SA/CMXG hydrogel (Scheme 1) was separated from the liquor, washed with distilled water, and then dried in an oven at 60 °C.[23]

In situ *preparation of crosslinked SA/CMXG/AgNP composites*

Equal quantities of both SA and CMXG (1 g) were stirred in deionized water (100 mL) till complete dissolution. To the obtained homogenous solution, silver nitrate solution (10 mL) was gradually added and stirred at 50 °C for 3 h. The color of the reaction mixture gradually changed to brown as a result of the green reduction of Ag+ ions to silver nanoparticles (AgNPs) by the action of the OH groups on the polymers' backbone. Afterwards, $CaCl_2$ solution (50 mL, 0.05 mol/L) was gradually added to the reaction solution with constant stirring till complete precipitation of the SA/CMXG/AgNPs composite, which was filtered, washed with water and dried in the oven for 6 h at 60 °C. Two different concentrations of silver nitrate (1 wt% and 3 wt% based on the total polymers' weight in the blend) were used to obtain two AgNP composites, designated as SA/CMXG/AgNPs1% and SA/CMXG/AgNPs3%, respectively. Scheme 2 shows the steps of preparation of SA/CMXG/AgNPs composite.[16,20]

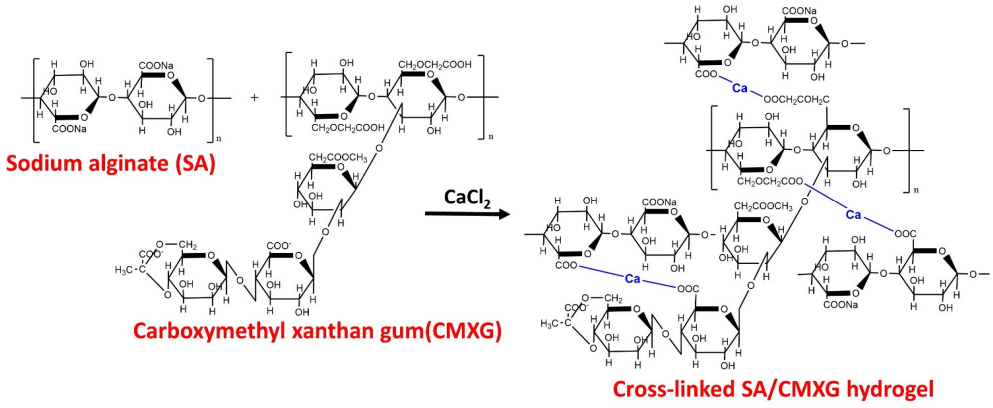

Scheme 1: Structure of the crosslinked SA/CMXG hydrogel

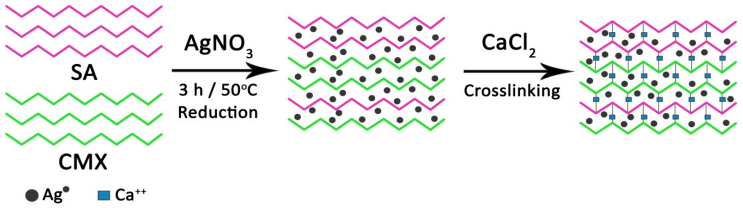

Scheme 2: Schematic representation of preparation of SA/CMXG/AgNPs composite

In vitro *Cyclooxygenase (COX) inhibition assay*

The evaluation of the capacity of the crosslinked SA/CMXG hydrogel and its AgNP composites for inhibition of ovine COX-2 (IC_{50} values, mM) was carried out using an enzyme immunoassay (EIA) kit (catalog number 560101, Cayman Chemical, Ann Arbor, MI, USA). Prostaglandin H2 (PGH2) was catalyzed by Cyclooxygenase in the first stage of the arachidonic acid (AA) biosynthesis. The measurement of PGF2a, synthesized from PGH2, was performed using the enzyme immunoassay (ACE competitive EIA) by $SnCl_2$ reduction. In brief, to 960 µL of buffer solution (0.1 M Tris HCl, pH 8.0, containing 5 mM EDTA and 2 mM phenol) 10 µL of COX-2 enzyme, in the presence of 10 µL of heme, were added. This assay depended on the competition between PGs and a PG-acetylcholinesterase conjugate (PG tracer), for a little quantity of antiserum of PG. The complex of the antibody-PG linked with a mouse anti-rabbit monoclonal antibody, which was earlier tied to the well. Cleaning of the plate was done to get rid of unbounding reagents, and afterwards the Ellman reagent, which contains acetylcholine esterase substrate, was added to the well. A characteristic yellow color was produced from this enzymatic reaction, which was measured spectrometrically at 406 nm. The color intensity is proportional with the quantity of PG tracer linked to the well, which is inversely proportional to the quantity of PGs existing in the well during the incubation: Absorbance of [PG Tracer bound] a1/PGs. The inhibition (%) was measured by comparing samples treated with different control incubations. The sample concentration that induces 50% inhibition (IC_{50}, mM) was determined from the curve of the concentration inhibition response (duplicate determinations).[28,29]

Cytotoxicity evaluation using viability assay

For the cytotoxicity assay, in 100 µL of growth medium, normal human lung fibroblast cells (WI-38 cell line) were seeded at a cell concentration of $1x10^4$ cells per well in a 96-well plate. Serial doubling dilutions of the chemical compound tested were added to the convergent cell monolayers dispensed in 96 well, flat-bottomed microliter plates (Falcon, NJ, USA), with a multichannel pipette. For each test sample concentration, three wells were used, the control cells were incubated without a test sample, with or without DMSO. The little percentage of DMSO present in the wells (maximal 0.1%) was found not to affect the experiment; the yield of viable cells was determined by the colorimetric method after incubation of the cells. All experiments were performed in triplicates and a calculation was made of the cell cytotoxic effect of each tested compound. The optical density was determined using a microplate reader (SunRise, TECAN, Inc, USA) to assess the number of viable cells and the viability percentage was calculated as [(ODt/ODc)] x100 percent, where ODt is the mean optical density of wells treated with the sample and ODc is the mean optical density of untreated cells. The cytotoxic concentration (CC50), the concentration needed to cause toxic effects in 50% of intact cells, was determined for each concentration from graphic plots of the dose response curve, using Graphpad Prism (San Diego, CA. USA) software.[30]

Measurements

A Tescan Shimadzu FTIR spectrophotometer (Model 8000, Japan) was used for recording the FTIR spectra of the crosslinked SA/CMXG hydrogel and its AgNP composites in the range of 400–4000 cm^{-1} utilizing potassium bromide discs.

Brucker's D-8 Advanced Wide-Angle X-ray diffractometer was employed to inspect the inner entities of the crosslinked SA/CMXG hydrogel and its AgNP composites. The samples were scanned at a diffraction angle from 4^o to 60^o at a speed of 8^o min^{-1}.

A Hitachi Scanning Electron Microscope (SEM) (Model S-450) was utilized for observing the surface and porosity of the crosslinked SA/CMXG hydrogel and its AgNP composites. The samples were coated with sputtering gold before their photographing.

A Transmission Electron Microscope (JEM-HR-JEOL-JEM 2100) was used to inspect the morphological structure of the suspended solution of the SA/CMXG/AgNPs3% composite.

RESULTS AND DISCUSSION

Preparation of crosslinked SA/CMXG hydrogel and its AgNP composites

A new crosslinked SA/CMXG hydrogel was prepared by blending an equivalent weight ratio of SA and CMXG, followed by crosslinking the

yielded blend using calcium chloride at room temperature (Scheme 1). To modify the characteristics of the prepared hydrogel, two AgNP composites were prepared. This is achieved by heating an equivalent weight ratio of SA and CMXG together with $AgNO_3$ at 50 °C with continuous stirring for 3 h, followed by crosslinking using $CaCl_2$ solution. The reaction included reduction of the Ag ions to Ag metal nanoparticles by the action of the OH groups on the polymers backbone (Scheme 2). Two different concentrations of silver nitrate (1 wt% and 3 wt% based on the total polymers weight in the blend) were used to obtain two AgNP composites designated as SA/CMXG/AgNPs1% and SA/CMXG/AgNPs3%, respectively.

Characterization of crosslinked SA/CMXG hydrogel and its AgNP composites

FTIR spectroscopy

Figure 1(a) shows the FTIR spectra of CMXG and SA. For CMXG, the following absorption peaks were displayed: (1) at around 3421 cm^{-1} (intensive and broad), corresponding to the hydrogen bonded OH of alcoholic and carboxylic groups; (2) at 2847-2913 cm^{-1}, related to the stretching vibration of the C-H bond (symmetrical and asymmetrical); (3) at 1617 and 1537 cm^{-1}, assigned to the stretching vibration of the C=O group of the carboxylic groups (symmetrical and asymmetrical); (4) at 1438 cm^{-1}, attributed to the bending vibration of the C-H bond; (5) at 1379 cm^{-1}, referring to the free CH_3 of the acetate group; (6) at 1147 and 1099 cm^{-1}, ascribed to the C-O of the ester and carboxylic groups; (7) at 1011 cm^{-1}, related to the C-OH groups; and (8) at 617 cm^{-1}, referring to the C-H out-of-plane bending vibration.[31] For SA, the following absorption peaks appeared: (1) at around 3435 cm^{-1} (strong and broad), related to the stretching vibration of the hydrogen bonded OH groups; (2) at 2928 cm^{-1}, attributed to the stretching vibration of the C-H groups; (3) at 1616 cm^{-1} (strong), corresponding to the symmetric C=O vibration of the carboxylate groups; (4) at 1420 cm^{-1} (strong), due to the C-H bending vibration overlapped with the asymmetric vibration of the C=O groups; (5) at 1091 and 1031 cm^{-1}, assigned to C-O of carboxylate and alcoholic groups, respectively. The peak of lower intensity at 944 cm^{-1} referred to the overlapped -C-C-H, C-OH (bending) and C-O groups, while that at 619 cm^{-1} represented the C-H out-of-plane bending vibration.[32]

The FTIR spectra of crosslinked SA/CMXG hydrogel and its AgNP composites are represented in Figure 1(b). The crosslinked CMXG/SA hydrogel combined the bands of both SA and CMGX, with a shift of some vibrations to lower frequencies, as a result of crosslinking with Ca(II) ions. The peak that corresponded to C-O of ester at 1147 cm^{-1} shifted to 1117 cm^{-1}, whereas the peak that related to the carboxylic OH group at 1099 cm^{-1} shifted to 1040 cm^{-1}.

The results of FTIR analysis for SA/CMXG/AgNPs1% and SA/CMXG/AgNPs3% clearly revealed the presence of a shift in the peak vibration frequency of the OH groups to a lower value, due to the electrostatic interaction between the AgNPs and the OH groups of the crosslinked SA/CMXG hydrogel matrix, as illustrated in Figure 1(b). The peak at 3432 cm^{-1}, related to the hydrogen bonded OH, shifted to 3415 and 3404 cm^{-1} and that at 1040 cm^{-1} shifted to 1034 and 1030 cm^{-1}, while the peak related to the C-O of the carboxylate groups at 1117 cm^{-1} shifted to 1116 and 1112 cm^{-1} in the spectra of SA/CMXG/AgNPs1% and SA/CMXG/AgNPs3%, respectively. It seems that the hydrogel function groups enclosed the Ag nanoparticles *via* electrostatic interaction and van der Waals forces into the hydrogel matrix. This confirms the formation of the nanocomposites.[16,21]

Powder X-ray diffraction (XRD)

The XRD technique was employed to investigate the inner structure of the polymers individually, their blend crosslinked with Ca(II) ions and the composites with AgNPs, as shown in Figure 2. Both SA and CMXG showed a crystalline inner structure, resulting from the formation of a lot of hydrogen bonds between the polymer chains. Two crystalline peaks at 2Θ = 13.7º and 23.0º appeared in the XRD pattern of SA, whereas the pattern of CMXG showed two relatively low intensity crystalline peaks at 2Θ = 20.43º and 34.1º. These peaks completely disappeared after crosslinking with Ca(II) ions and the crosslinked SA/CMXG hydrogel has a completely amorphous inner structure. This may be attributed to the destruction of the inter- and intra-chain hydrogen bonds after crosslinking the polymeric chains with Ca(II) ions, resulting in an increase in the inner space between the chains of the polymers. The existence of AgNPs in the XRD patterns of the AgNP composites is confirmed by the appearance of the new peaks at 2θ = 27.8º, 32.19º, 46.13º and 56.0º,

corresponding to (1 1 1), (2 0 0) and (142) planes of the face centered cubic crystal structure of silver metal.[33]

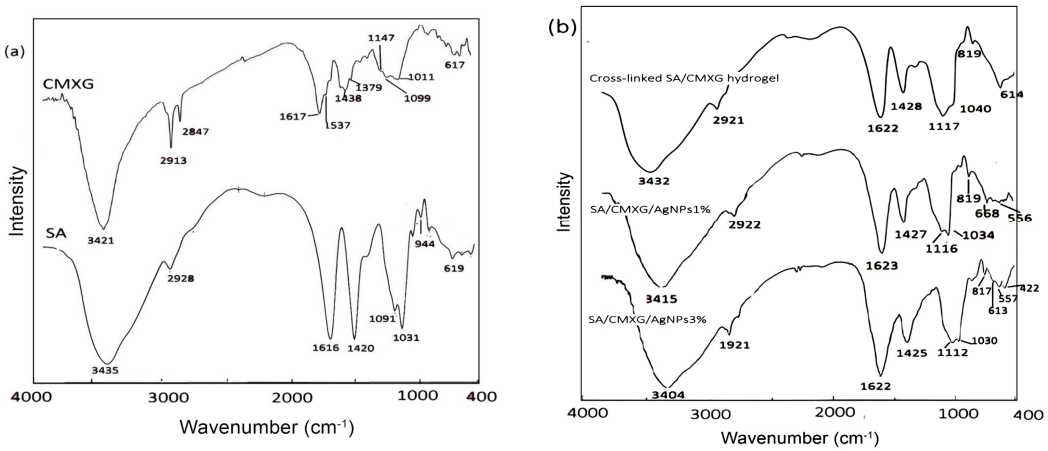

Figure 1: FTIR spectra of (a) SA and CMXG, and (b) crosslinked SA/CMXG hydrogel and its AgNP composites

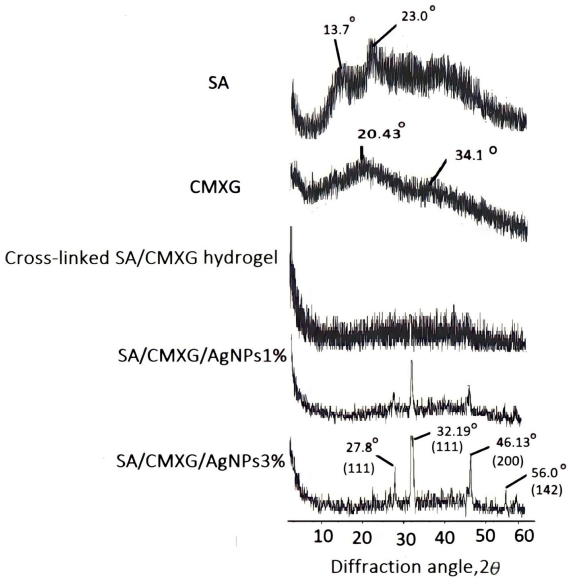

Figure 2: XRD patterns of the SA, CMXG, crosslinked SA/CMXG hydrogel and its AgNP composites

Scanning electron microscopy (SEM)

The fine structure and the surface morphology of the CMXG, SA, crosslinked SA/CMXG hydrogel and its AgNP composites were inspected using SEM (Fig. 3). The SEM images of unblended CMXG and SA showed a compact surface, with a bulk of lumps, because of the presence of a high number of intra- and inter-chain hydrogen bonds. Crosslinking of CMGX and SA with Ca(II) ions in the crosslinked SA/CMXG hydrogel destroys a significant amount of these hydrogen bonds, thus separates the chains from each other and creates a great number of pores spread along the hydrogel matrix. The SEM images of SA/CMXG/AgNP1% and SA/CMXG/AgNP3% composites show uniform distribution of *in situ* generated AgNPs in the composite matrix. The density of the dispersed AgNPs on the surface SA/CMXG/AgNP3% is more than that on SA/CMXG/AgNP1%. The homogenous dispersion of AgNPs as light spherical spots, without agglomeration or aggregation into the polymeric substrate, indicates the high efficiency

of the polymeric substrate to stabilize of the AgNPs. This may be ascribed to the interaction between the functional groups on the polymer matrix and AgNPs *via* van der Waals forces, resulting in an adequate homogeneous distribution of the created AgNPs. Thus, SEM analysis confirms the *in-situ* formation of the AgNPs.

Additionally, the energy dispersive X-ray spectroscopy (EDX) was performed during SEM observations to detect the elements in the SA/CMXG/AgNP composites. The EDX diagrams (Fig. 4) show the existence of the silver element in the SA/CMXG/AgNP composite matrix, with a silver weight percent of 4.43% in SA/CMXG/AgNPs3%, corresponding to 3.01% in SA/CMXG/AgNPs1%. The existence of other elements, such as C, O, Cl, Na and Ca, was also confirmed (Fig. 4).

Transmission electron microscopy (TEM)

An additional morphological observation of the nanocomposites using TEM was performed for describing the structural characteristics of the AgNPs inside the crosslinked SA/CMXG hydrogel matrix. Figure 5 (a and b) shows the TEM micrographs of the SA/CMXG/AgNPs3% composite, at different magnifications, in which the AgNPs appear in a spherical, regular shape, with different sizes, ranging from 13 to 26 nm. TEM micrographs also show uniform distribution, with no aggregation of the AgNPs inside the composite matrix, due to the attachment of AgNPs to the functional groups of the polymers. This indicated the stabilizing effect of the polymers on the silver nanoparticles. The homogeneous distribution and the particle size of the AgNPs in the hydrogel matrix is evidenced by atomic force microscopy images in Figure 6 (a and b).

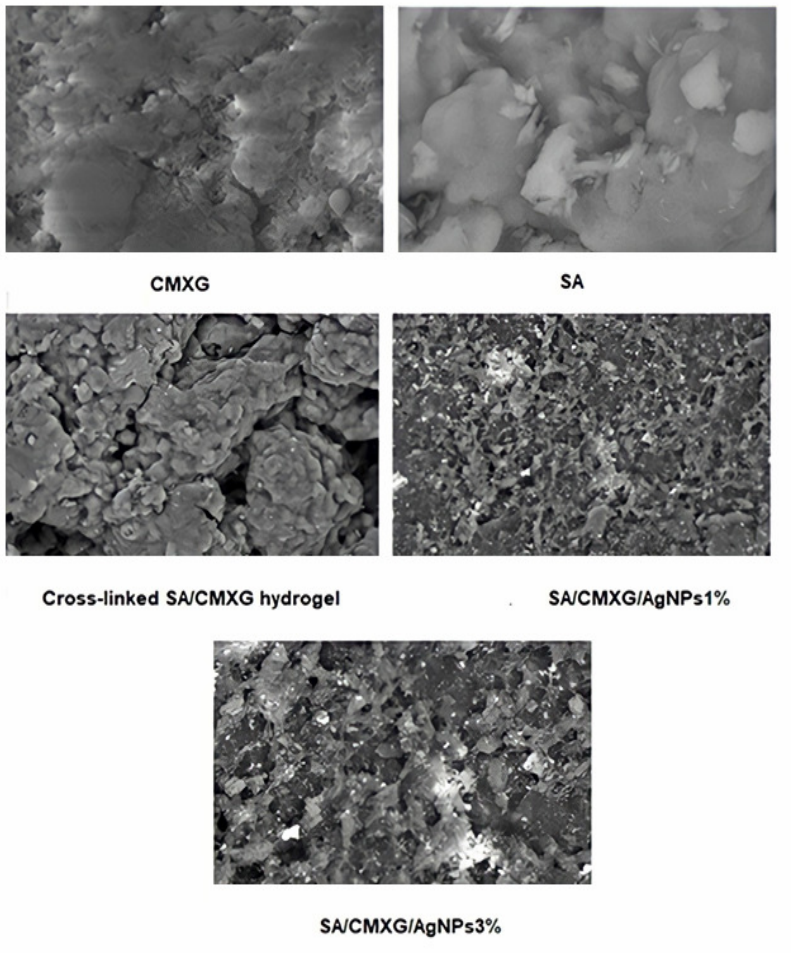

Figure 3: SEM images of CMXG, SA, crosslinked SA/CMXG hydrogel and its AgNP composites at 8000x magnification

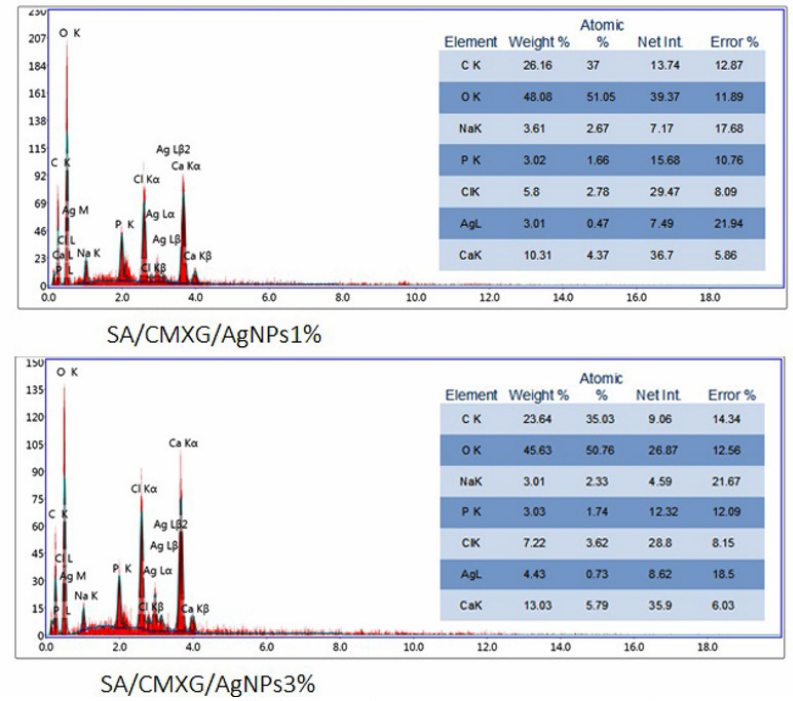

Figure 4: EDX patterns of SA/CMXG/AgNP composites

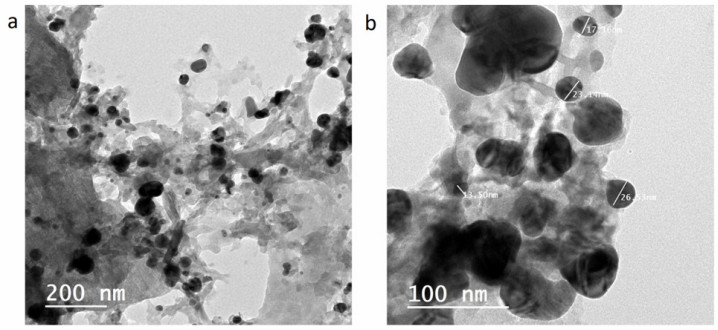

Figure 5: TEM images of SA/CMXG/AgNPs3% at different magnifications

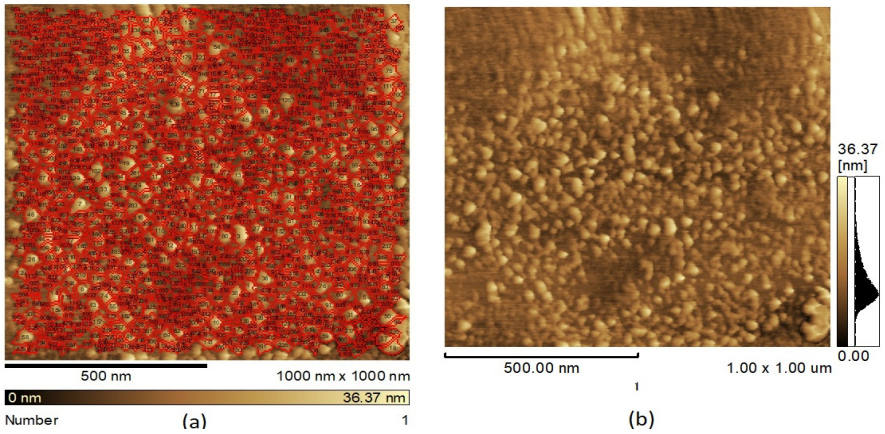

Figure 6: AFM images showing (a) particle size analysis of AgNPs, (b) homogeneous distribution of AgNPs inside the hydrogel matrix

Evaluation of *in vitro* anti-inflammatory activity of crosslinked SA/CMXG hydrogel and its AgNP composites against COX-2

The prostaglandins are a class of lipid compounds that have physiological activity. They are called eicosanoids and have varied effects like hormones in animals. Prostaglandins exist in almost each tissue of humans and animals. Enzymatically, prostaglandins originate from the arachidonic fatty acid. They are the main metabolites of the cyclooxygenase enzymes (COX), which are found in two different isoforms: COX-1 and COX-2. It is believed that COX-1 is accountable for regulation of the tissues' normal physiological functions, whereas COX-2 is inducible in fibroblasts, macrophages, as well as sundry other cell types by pro-inflammatory stimuli.[34,35] Moreover, COX-2 is accountable for producing large quantities of pro-inflammatory prostaglandin at the sites of inflammation.

Inflammation represents the complex response of the immune system to infections and injuries. This leads to removing the offending factors and regaining both the structure and physiological function of the tissues.[36] The inflammation symptoms display as heat, pain, swelling, redness and functional loss. They are categorized, based on the inflammatory interaction duration, into two main types: acute or chronic. Although they start as a protective phenomenon, regulation loss of this complex process results in developing different inflammatory disorders.

Amongst the wide variety of available nanoparticles, AgNPs have attracted much attention due to their distinct biological activities for prospective applications. Silver was anciently utilized to treat inflammations and wounds. AgNPs were developed to have potent antioxidant properties[37] and efficient anti-inflammatory activity.[38,39]

Due to the weak biological properties of both alginate and xanthan gum, they have been modified *via* inclusion of antimicrobial nanoparticles, for example AgNPs, or by incorporating antimicrobial moieties[32,40-42] into their matrices to improve their anti-inflammatory and antimicrobial properties.

In this study, the anti-inflammatory effect of SA/CMXG/AgNPs was evaluated by calculating the value of inhibition against the COX-2 enzyme, which is responsible for inflammation in the human body. Figure 7 shows the behavior of the tested samples against COX-2 enzyme activity. The analysis revealed that the order of COX-2 inhibition by the tested samples was SA < CMXG < crosslinked SA/CMXG hydrogel < SA/CMXG/AgNPs1% < SA/CMXG/AgNPs3% < Celecoxib. It is observed that the crosslinked SA/CMXG hydrogel has a significant inhibitory activity, compared with its individual components (SA and CMXG), while its AgNP composites exhibit a potent inhibition tendency and their activity increased with increasing the AgNPs content. The recorded MIC values revealed that the values that cause 50% inhibition (IC_{50}) of COX-2 enzyme activity were 14.2 and 3.6 µg/mL for SA/CMXG/AgNPs1% and SA/CMXG/AgNPs3%, respectively, corresponding to 0.28 µg/mL for the standard drug Celecoxib, as illustrated in Table 1. Thus, these nanocomposites can be regarded as promising natural ant-inflammatory agents.

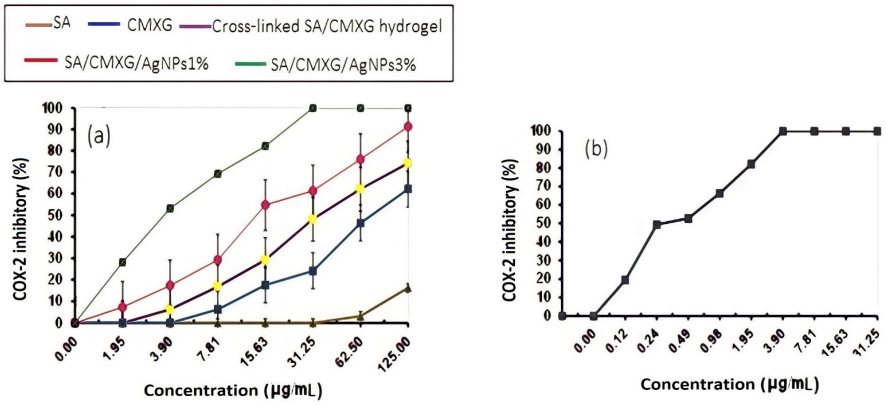

Figure 7: Anti-inflammatory activity against COX-2 of: (a) SA, CMXG, crosslinked SA/CMXG hydrogel and its AgNP composites, and (b) standard drug Celecoxib

Table 1
IC_{50} of samples against COX-2 activity

Samples	IC_{50} (µg/mL)
SA	>125
CMXG	76.9
Crosslinked SA/CMXG hydrogel	26.8
SA/CMXG/AgNPs1%	14.2
SA/CMXG/AgNPs3%	3.6
Celecoxib	0.28

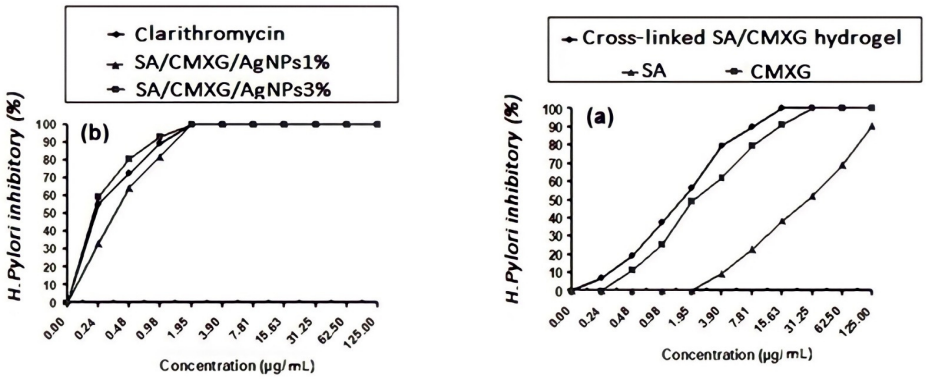

Figure 8: Anti-*H. pylori* activity of (a) SA, CMXG and SA/CMXG hydrogel, and (b) SA/CMXG/AgNP composites and standard drug Clarithromycin

Table 2
Minimum inhibitory concentration (MIC) of the tested samples against *H. pylori*

Samples	MIC (µg/mL)
SA	>125
CMXG	31.25
Crosslinked SA/CMXG hydrogel	15.81
SA/CMXG/AgNPs1%	3.9
SA/CMXG/AgNPs3%	1.95
Clarithromycin	1.95

Crosslinked SA/CMXG hydrogel and its AgNP composites as potential *anti-Helicobacter pylori* agents

The activity of SA, CMXG, crosslinked SA/CMXG hydrogel and its AgNP composites against *H. pylori* was determined by the micro-well dilution method, using the tetrazolium salt (MTT) assay to evaluate *H. pylori* proliferation. It depends on the change of MTT color, which is a measure to the metabolic activity of bacterial cells. The reduction of the purple color is an indication of better inhibitory activity of the tested samples. The results of SA, CMXG and crosslinked SA/CMXG hydrogel shown in Figure 8 and Table 2 indicate that the crosslinked SA/CMXG hydrogel has a higher inhibition activity towards the growth of *H. pylori* than its individual components (SA and CMXG). Meanwhile, the minimum inhibitory concentration (MIC) value that resulted in 100% growth inhibition of *H. pylori* was 15.81 µg/mL for the crosslinked SA/CMXG hydrogel, compared to 31.25 and >125 µg/mL for CMXG and SA, respectively (Table 2).

On the other hand, the SA/CMXG/AgNPs1% and SA/CMXG/AgNPs3% exhibited 100% inhibition against *H. pylori* growth at MIC of 3.9 µg/mL and 1.95 µg/mL, respectively, compared to 15.81 µg/mL for the crosslinked SA/CMXG parent hydrogel (Table 2). It is worth mentioning that the anti-*H. pylori* activity of SA/CMXG/AgNPs3% was higher than that of the standard drug

Clarithromycin, especially at low concentrations ranging from 0.24 to 0.98 µg/mL. These results make SA/CMXG/AgNP composites promising anti-*H. pylori* agents.

Evaluation of cytotoxicity of SA/CMXG/AgNPs3% on normal human cells

The cytotoxic activity of the SA/CMXG/AgNPs3% composite was studied against normal human lung fibroblast cells (WI-38 cell line), using concentrations ranging from 0 to 500 µg/mL (Table 3). The results showed that the viability of the normal cells is affected by SA/CMXG/AgNPs-3% at a concentration of 15.6 µg/mL, while it had no inhibitory activity below this concentration. The half calculated cytotoxic concentration (CC_{50}), the concentration causing toxic effects in 50% of intact cells, for SA/CMXG/AgNPs3% was 93 ± 2.62 µg/mL. From Tables 1 and 2, it was deduced that the nanocomposite SA/CMXG/AgNPs3% exhibited high COX-2 activity and anti-*H. pylori* activity, with MIC values lower than the cytotoxic concentrations of the composite (15.6 µg/mL), indicating that these Ag nanocomposites are safe for normal human cells and can be used with high efficiency as anti-inflammatory and anti-*Helicobacter pylori* agents in biological application. Microscopic examination of normal human lung fibroblast cells incubated for 24 h with SA/CMXG/AgNPs3% samples at 62.5 µg/mL is shown in Figure 9.

Table 3
Inhibitory activity of SA/CMXG/AgNPs3% against human lung fibroblast normal cells (WI-38 cell line)

Sample conc. (µg/mL)	Viability (%)	Inhibition (%)	SD (±)
500	10.93	89.07	1.89
250	23.17	76.83	2.71
125	38.65	61.35	3.47
62.5	61.49	38.51	2.35
31.25	83.18	16.82	1.46
15.6	96.41	3.59	0.83
0	100	0	0

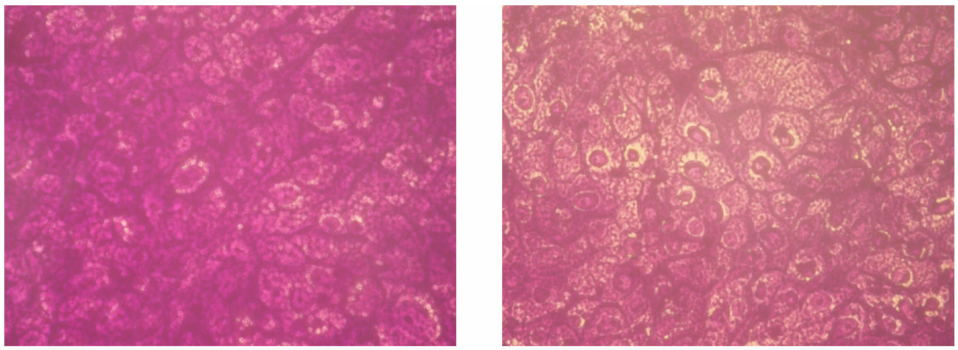

Figure 9: Microscope examination of normal human lung fibroblast cells (WI-38 cell line) incubated with SA/CMXG/AgNPs3% samples at 62.5 µg/mL for 24 h, compared with untreated cells (control cells)

CONCLUSION

A blend composed of an equivalent weight ratio of SA and CMXG was successfully crosslinked using $CaCl_2$ to obtain a crosslinked SA/CMXG hydrogel. Two AgNP bio-composites were also prepared by *in situ* dispersion of two different concentrations of AgNPs into the matrix of the prepared hydrogel. FTIR, XRD, SEM, EDX and TEM techniques were utilized to confirm the structure of the hydrogel and its AgNP composites. The analysis displayed that the order of COX-2 inhibition by the tested samples was SA < CMXG < crosslinked SA/CMXG hydrogel < SA/CMXG/AgNPs1% < SA/CMXG/AgNPs3% < Celecoxib. AgNP composites exhibited a potent inhibition tendency and their activity increases with increasing the AgNPs content. The recorded MIC values revealed that the MIC values that cause 50% inhibition (IC_{50}) of COX-2 enzyme activity was 14.2 and 3.6 µg/mL for SA/CMXG/AgNPs1% and SA/CMXG/AgNPs3%, respectively,

corresponding to 0.28 µg/mL for the standard drug Celecoxib. SA/CMXG hydrogel exhibited higher inhibition efficiency against *H. pylori* than its individual components (CMXG and SA). Only 15.81 µg/mL of SA/CMXG hydrogel is sufficient to kill 100% of the *H. pylori*, while the concentrations of CMXG and SA were 31.25 and >125 µg/mL, respectively. Furthermore, SA/CMXG/AgNP composites are more potent in inhibiting *H. pylori* than their parent SA/CMXG hydrogel. The inhibition efficiency increased with increasing the AgNPs content – only 3.9 and 1.95 µg/mL of SA/CMXG/AgNPs1% and SA/CMXG/AgNPs3%, respectively, can inhibit 100% of the *H. pylori* growth. SA/CMXG/AgNPs 3% was found to be more potent in inhibiting *H. pylori* than the standard drug Clarithromycin, especially at low concentrations ranging from 0.24 to 0.98 µg/mL. These results make SA/CMXG/AgNPs3% a promising anti-*H. pylori* agent. Thus, it can be concluded that the integration of SA, CMXG and AgNPs into one system results in a remarkable enhancement in efficiency, in comparison with that of both SA and CMXG taken individually. These findings open the way for acquiring promising systems that could compete with classical antibiotic drugs.

ACKNOWLEDGMENT: The authors are thankful to the Deanship of Scientific Research at Najran University for funding this work through the research grant NU/-/SERC/10/546.

REFERENCES

[1] N. Tharmalingam, J. Port, D. Castillo and E. Mylonakis, *Sci. Rep.*, **8**, 3701 (2018), https:/doi.org/10.1038/s41598-018-22037-x
[2] A. G. Gravina, R. M. Zagari, C. De Musis, L. Romano *et al.*, *World J. Gastroenterol.*, **24**, 3204 (2018), https:/doi.org/10.3748/wjg.v24.i29.3204
[3] S. J. Desai, B. Prickril and A. Rasooly, *Nutr. Cancer.*, **70**, 350 (2018), https:/doi.org/10.1080/01635581.2018.1446091
[4] Z. Ju, *Acta Pharm. Sin. B*, **12**, 2700 (2022)
[5] Y. Wang, J. Zhang, M. Li, M. Li, S. Xie *et al.*, *Chem. Biol. Drug Des.*, **89**, 670 (2017), https:/doi.org/10.1111/cbdd.12888
[6] P. Rajendran, Y. F. Chen, Y. F. Chen, L. C. Chung, S. Tamilselvi *et al.*, *J. Cell. Physiol.*, **233**, 6458 (2018), https:/doi.org/10.1002/jcp.26479
[7] R. J. Flower, *Nat. Rev. Drug Discov.*, **2**, 179 (2003), https:/doi.org/10.1038/nrd1034
[8] M.-Y. Song, D.-Y. Lee and E.-H. Kim, *J. Microbiol.*, **58**, 878 (2020), https:/doi.org/10.1007/s12275-020-0277-z
[9] S. Ansari and Y. Yamaoka, *J. Clin. Med.*, **11**, 3141 (2022), https:/doi.org/10.3390/ jcm11113141
[10] J. C. Sierra, S. Hobbs, R. Chaturvedi, F. Yan, K. Wilson *et al.*, *Am. J. Physiol. Gastrointest. Liver Physiol.*, **305**, G196 (2013), https:/doi.org/10.1152/ajpgi.00495.2012
[11] J. K. Patra, G. Das, L. F. Fraceto, E. V. R. Campos, M. del Pilar Rodriguez-Torres *et al.*, *J. Nanobiotechnol.*, **16**, 71 (2018), https:/doi.org/10.1186/s12951-018-0392-8
[12] S. Sim and N. K. Wong, *Biomed. Rep.*, **14**, 1 (2021), https:/doi.org/10.3892/br.2021.1418
[13] E. M. Egorova, A. A. Kubatiev and V. I. Schvets, "Biological Effects of Metal Nanoparticles", Springer, Switzerland, 2016, https:/doi.org/10.1007/978-3-319-30906-4
[14] C. Tyavambiza, A. M. Elbagory, A. M. Madiehe, M. Meyer and S. Meyer, *J. Nanomater.*, **11**, 1343 (2021), https:/doi.org/10.3390/nano11051343
[15] X.-F. Zhang, Z.-G. Liu, W. Shen and S. Gurunathan, *Int. J. Mol. Sci.*, **17**, 1534 (2016), https:/doi.org/10.3390/ijms17091534
[16] J. Yang, H. Zheng, S. Han, Z. Jiang and X. Chen, *RSC Adv.*, **5**, 2378 (2015), https:/doi.org/10.1039/C4RA12836B
[17] Y. Qing, L. Cheng, R. Li, G. Liu, Y. Zhang *et al.*, *Int. J. Nanomed.*, **13**, 3311 (2018), https:/doi.org/10.2147/IJN.S165125
[18] A. Kubyshkin, D. Chegodar, A. Katsev, A. Petrosyan, Y. Krivorutchenko *et al.*, *Biochem. Mol. Biol. Int.*, **2**, 1 (2016), https:/doi.org/10.21767/2471-8084.100022
[19] J. Jeevanandam, A. Barhoum, Y. S. Chan, A. Dufresne and M. Danquah, *Beilstein J. Org. Chem.*, **9**, 1050 (2018), https:/doi.org/10.3762/bjnano.9.98
[20] J. Huang, J. Ren, G. Chen, Y. Deng, G. Wang *et al.*, *J. Nanomater.*, **2017**, 6802397 (2017), https://doi.org/10.1155/2017/6802397
[21] W. Xu, W. Jin, L. Lin, C. Zhang, F. Y. Quan *et al.*, *Carbohyd. Polym.*, **101**, 961 (2014), https:/doi.org/10.1039/c5ra07821k
[22] Y. Han, M. Yu and L. Wang, *Food Packag. Shelf Life*, **15**, 35 (2018), https:/doi.org/10.5772/intechopen.80707
[23] Z. Li and Z. Lin, *Aggregate*, **2**, 21 (2021), https:/doi.org/10.1002/agt2.21
[24] A. M. Elgamal, M. H. A. Elella, G. R. Saad and N. A. Abd El-Ghany, *Mater. Today Commun.*, **33**, 104209 (2022), https:/doi.org/org/10.1016/j.mtcomm.2022.104209
[25] R. Mohammadinejad, A. Kumar, M. Ranjbar-Mohammadi and M. Ashrafizadeh, *Polymers*, **12**, 176 (2020), https:/doi.org/10.3390/polym12010176
[26] M. Szekalska, A. Puciłowska, E. Szymańska, P. Ciosek and K. Winnicka, *Int. J. Polym. Sci.*, **2016**, 1 (2016), https:/doi.org/10.1155/2016/7697031
[27] M. Ahuja, A. Kumar and K. Singh, *RSC Adv.*, **10**, 27103 (2020), https:/doi.org/10.1039/d0ra04366d

[28] A. A.-M. Abdel-Aziz, A. S. El-Azab, N. A. AlSaif, M. M. Alanazi, M. A. El-Gendy *et al*., *J. Enzyme Inhib. Med. Chem.*, **35**, 610 (2022), https:/doi.org/10.1080/14756366.2020.1722120
[29] Z. Chen, L. Xing, Q. Fan, A. G. Cheetham, R. Lin *et al*., *Theranostics*, **7**, 2003 (2017), https:/doi.org/10.7150/thno.19404
[30] N. A. Abd El-Ghany and Z. M. Mahmoud, *Polym. Bull*., **78**, 6161 (2021), https:/doi.org/10.1007/s00289-020-03417-8
[31] A. Mohsin, K. Zhang, J. Hu, S. Rehman, M. Tariq *et al*., *Carbohyd. Polym*., **181**, 793 (2018), https:/doi.org/10.1016/j.carbpol.2017.11.076
[32] M. A. Elella, M. M. Abdel-Aziz and N. A. Abd El-Ghany, *Cellulose Chem. Technol*., **55**, 75 (2021), https://doi.org/10.35812/CelluloseChemTechnol.2021.55.08
[33] N. Y. Elmehbad and N. A. Mohamed, *Int. J. Biol. Macromol*., **151**, 92 (2020), https:/doi.org/10.1016/j.ijbiomac.2020.01.298
[34] A. S. El-Azab, A. A.-M. Abdel-Aziz, L. A. Abou-Zeid, W. M. El-Husseiny, A. M. El-Morsy *et al*., *J. Enzyme Inhib. Med. Chem.*, **33**, 989 (2018), https:/doi.org/10.1080/14756366.2018.1474878
[35] N. A. Mohamed, N. A. Abd El-Ghany and M. M. Abdel-Aziz, *Int. J. Biol. Macromol*., **181**, 956 (2021), https:/doi.org/10.1016/j.ijbiomac
[36] A. K. Mani, S. Seethalakshmi and V. Gopal, *J. Nanomed. Nanotechnol*., **6**, 1 (2015), https:/doi.org/10.4172/2157-7439.1000268
[37] I. Murali Krishna, G. Bhagavanth Reddy, G. Veerabhadram and A. Madhusudhan, *Appl. Nanosci*., **6**, 681 (2016), https:/doi.org/10.1007/s13204-015-0479-6
[38] J. J. Martínez-Sanmiguel, D. G Zarate-Triviño, R. Hernandez-Delgadillo, A. L. Giraldo-Betancur, N. Pineda-Aguilar *et al*., *J. Biomater. Appl*., **33**, 1314 (2019), https:/doi.org/10.1177/0885328219835995
[39] P. Singh, S. Ahn, J.-P. Kang, S. Veronika, Y. Huo *et al*., *Artif. Cells Nanomed. Biotechnol*., **46**, 2022 (2018), https:/doi.org/10.1080/21691401.2017.1408117
[40] K. Rao, S. Aziz, T. Roome, A. Razzak, B. Sikandar *et al*., *Artif. Cells Nanomed. Biotechnol*., **46**, 597 (2018), https:/doi.org/10.1080/21691401.2018.1431653
[41] N. A. A. El-Ghany and M. A. H. Elella, in "Food Packaging: Safety, Management and Quality", edited by W. F. Lai, New York, Nova Science Publishers, Inc., 2022, https:/doi.org/10.52305/SEPV4757
[42] A. M. Elgamal, N. A. Abd El-Ghany and G. R. Saad, *J. Appl. Polym. Sci*., **139**, e53179 (2022), https:/doi.org/10.1002/app.53179